A note on the modelling of lubrication forces in unresolved simulations

Nijssen, Tim M.J.; Ottens, Marcel; Padding, Johan T.

Important note
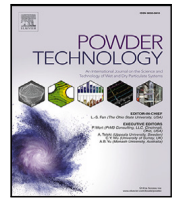To cite this publication, please use the final published version (if applicable).
Please check the document version above.

Short communication

A note on the modelling of lubrication forces in unresolved simulations

Tim M.J. Nijssen [a,*], Marcel Ottens [a], Johan T. Padding [b]

[a] *Delft University of Technology, Department of Biotechnology, Van der Maasweg 9, 2629 HZ, Delft, The Netherlands*
[b] *Delft University of Technology, Faculty of Mechanical, Maritime and Materials Engineering, Department of Process & Energy, Complex Fluid Processing, Leeghwaterstraat 39, 2628 CB, Delft, The Netherlands*

HIGHLIGHTS

- A rigorously-defined lubrication force model for unresolved simulations is proposed.
- Surface roughness and particle deformation are considered.
- Numerical stability is ensured by a continuous force formulation.
- Good correspondence with experimental data is demonstrated.

GRAPHICAL ABSTRACT
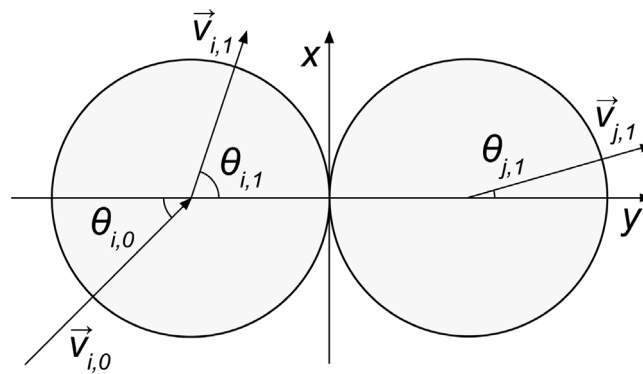
ARTICLE INFO

ABSTRACT

Lubrication forces play a major role in the behaviour of fluid–solid systems, where they affect the collisions between particles. Current implementations of lubrication forces in unresolved simulations often suffer from shortcomings, such as neglecting parts of the physics or relying on arbitrarily defined parameters. In this short communication, we propose a novel implementation, rigorously defined based on physical and numerical factors. Both particle roughness and deformation are considered, and the model accuracy is demonstrated through comparison with experimental results.

1. Introduction

Unresolved simulation methods (e.g. CFD-DEM [1]) are powerful tools to study interacting fluid (gas or liquid) and particle phases. Contrary to fully-resolved simulations (e.g. [2–5]), in the unresolved methods the fluid flow is only evaluated at scales larger than the particles, relying on models to account for the sub-grid particle–fluid interaction, i.e. the drag force and possibly additional forces [6]. It is well-known that the lubrication forces arising during immersed collisions significantly influence the macroscopic behaviour of liquid–solid systems [7,8], and even gas–solid systems with sufficiently small and/or light particles [9]. Experimental work on liquid–solid fluidised

beds [7,10] has shown that fluid effects on particle interactions might lead to heterogeneity and either increase or decrease bed expansion. This complexity of these effects is reflected by the numerical literature, in which no consensus on the effect of lubrication forces on liquid–solid fluidised bed behaviour has been reached.

Many of the previously applied models rely on an effective restitution coefficient to account for the enhanced dissipation stemming from the lubrication forces. Liu et al. [8] implemented such a method and observed decreased expansion and granular temperature as results. Other researchers (e.g. [11,12]) have chosen to directly implement the lubrication force. This approach more accurately captures the physics

---

of the collision as it includes the increased interaction distance between the solid particles, but often relies on arbitrary cut-off distances to ensure numerical stability and/or computational speed. Campos et al. [11] observed increased heterogeneity within the bed, while through a similar approach Wang et al. [12] found a more homogeneous particle distribution resulting from lubrication forces. These contradictory findings illustrate that an accurate description of the lubrication forces and their effects on particle interactions is imperative to simulation of fluid–solid systems. Clearly, a universally-accepted method is currently unavailable, and would greatly benefit the scientific community. Such a method needs to combine accuracy, simplicity, numerical efficiency and robustness to be applicable in large many-body simulations. In this brief communication, we propose a novel implementation of lubrication forces for unresolved simulations, aiming to provide a rigorously defined method to be used in future work. The model is derived based on physical and numerical considerations, and compared with experimental data to demonstrate its accuracy.

2. Proposed model

The lubrication force is associated with the draining and filling of a thin fluid film between the surfaces of colliding solid bodies. The first solutions of it were presented by Brenner and Cox [13,14] in the 1960s. The normal lubrication force acting on two spherical bodies i and j can be described by Eq. (1), where η_f is the fluid viscosity, Δv_n the relative normal velocity, $R^* = R_i R_j / (R_i + R_j)$ the reduced radius, $h = |\vec{r}_{ij}| - R_i - R_j$ the height of the gap between the surfaces, and $|\vec{r}_{ij}|$ the vector between the particle centres.

$$F_{l,n} = -\frac{6\pi\eta_f \Delta v_n R^{*2}}{h} \tag{1}$$

In various experimental studies (e.g. [15]), the rebound of colliding particles in different media was studied. Consistently, a strong dependence of the restitution coefficient $e = |\Delta\vec{v}_1|/|\Delta\vec{v}_0|$ (0 and 1 denoting the approach and rebound, respectively) on the dimensionless Stokes number was observed. Here, we will employ the definition by Yang and Hunt [16] (Eq. (2), where $m^* = m_i m_j / (m_i + m_j)$ denotes the reduced mass of the bodies). For collisions below a critical Stokes number St_c, no rebound is observed. The exact value of St_c is unknown, but values in the range $5 \leq St_c \leq 20$ are commonly found (e.g. [16–18]). Conversely, at high Stokes number ($St > 2000$ [16]), influence of the interstitial medium is negligible. For accurate simulation of fluid–solid systems, it is of vital importance to accurately capture the transition between these two extremes.

$$St = \frac{m^*|\Delta\vec{v}_0|}{6\pi\eta_f R^{*2}} \tag{2}$$

2.1. Minimum approach

As seen from Eq. (1), the lubrication force diverges as h approaches zero. This leads to a paradox where two approaching bodies can never truly come into contact. This paradox relies on the assumption of perfectly rigid and smooth surfaces, which does not hold in practical examples. Joseph and Hunt [19] described that rigid, rough surfaces interact through their asperities, while sufficiently smooth and soft surfaces deform to maintain a finite minimum gap height $h^{\min}$. A solution for the latter case, the elastohydrodynamic collision, was derived by Davis et al. [20]. The deformation is governed by the elasticity parameter ε (Eq. (4) [20]), where $E^{*-1} = (1 - \nu_i^2)/E_i + (1 - \nu_j^2)/E_j$ is the reduced elastic modulus, ν is Poisson's ratio, and $\Delta v_{n,0}$ and h_0 denote the initial normal velocity and gap height). A third contact mechanism, glass transition of the liquid phase, was described by Donahue et al. [21]. We have not included this mechanism into our model, as it is not significant under the present conditions and introduces the glass transition pressure, a highly challenging parameter to obtain.
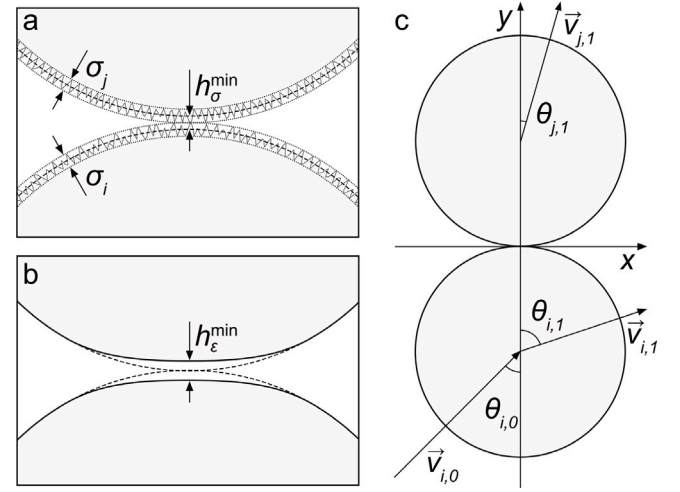

Fig. 1. Close-up of contact between rigid, rough particles (a), smooth, deformable particles (b) and collision geometry, indicating impact and rebound velocities and angles (c).

The approach distance of two rigid surfaces in contact through the tops of their asperities is given by the mean value of their roughness heights σ (Eq. (3), Fig. 1a). The minimum approach due to deformation is expressed by Eq. (5) [18] (Fig. 1b). To account for non-monotonous movement of the particles in simulations (e.g. due to interaction with other particles), the highest occurring normal velocity during the approach should be implemented as approach velocity $\Delta v_{n,0}$. The maximum value of both minimum approach distances is taken as the actual minimum approach distance of two rough, deformable particles (Eq. (6)).

$$h_\sigma^{\min} = \frac{\sigma_i + \sigma_j}{2} \tag{3}$$

$$\varepsilon = \frac{4\eta_f \Delta v_{n,0} R^{*\frac{3}{2}}}{\pi E^* h_0^{\frac{5}{2}}} \tag{4}$$

$$h_\varepsilon^{\min} \approx \frac{1}{3} h_0 \varepsilon^{\frac{2}{5}} \approx 0.37 \sqrt[5]{\left(\frac{\eta_f \Delta v_{n,0}}{E^*}\right)^2 R^{*3}} \tag{5}$$

$$h^{\min} = \max\left(h_\sigma^{\min}, h_\varepsilon^{\min}\right) \tag{6}$$

2.2. Normal force

Following the findings of Joseph and Hunt [19], the normal component of the lubrication force can be evaluated independently from the tangential component. The force exerted on two approaching particles is expressed by Eq. (8), where the gap height h is truncated to the minimum approach distance $h^{\min}$. This force is applied to any two particles with a separation smaller than a cut-off distance h^{co}, but larger than 0. Here, we used a cut-off distance of $h^{co} = R^*$, as suggested by Yang and Hunt [16]. If the two approaching particles overcome the lubrication force and collide, their interaction stemming from the deforming surfaces is described by an established contact model. In this work, the contact force $\vec{F}_c$ is evaluated through the Hertzian contact model, an extensive description of which can be found in the work of Di Renzo and Di Maio [22]. In a lubricated collision, the deformation of the surfaces already starts when the minimum approach distance $h^{\min}$ is reached. Therefore, the normal overlap δ_n is increased by $h^{\min}$, as shown in Eq. (7). For gap heights between $h^{\min}$ and 0, the total force between the particles is a combination of the lubrication force and the contact force, either through asperity contact or elastohydrodynamic deformation. In this transition zone, the total force is approximated by

a lever-type expression, which linearly evolves between the lubrication force $F_{l,n}$ and the contact force $F_{c,n}$. This simple expression ensures the total force remains continuous, which is important for application of the model in large-scale simulations, as sudden jumps of force might lead to unstable behaviour during numerical integration, demanding a small integration time step and impeding numerical efficiency. The resulting normal force is summarised by Eq. (9).

$$\delta_n = \max(0, h^{\min} - h) \tag{7}$$

$$F_{l,n} = -\frac{6\pi\eta_f \Delta v_n R^{*2}}{\max(h, h^{\min})} \tag{8}$$

$$F_n = \begin{cases} 0 & \text{for} & h > h^{co} \\ F_{l,n} & \text{for} & h^{\min} < h \le h^{co} \\ \frac{h}{h^{\min}} F_{l,n} + \frac{h^{\min}-h}{h^{\min}} F_{c,n} & \text{for} & 0 < h \le h^{\min} \\ F_{c,n} & \text{for} & h \le 0 \end{cases} \tag{9}$$

2.3. Tangential force

Besides the normal force, lubrication effects also play a role in the tangential interaction of bodies. Elaborate analytical expressions are available from O'Neill and Majumdar [23,24], but do not account for the roughness of the surfaces. Instead, we employ empirical approach more suited for large-scale simulations, based on the findings of Joseph and Hunt [19], who extended their experimental work on particle–wall impacts by performing oblique collisions. By observing the rebound angle, they were able to determine the coefficient of friction μ_f. The tangential component of the collision was found to behave much like a dry collision, with a drastically reduced friction coefficient in cases where a thin fluid film remains between the surfaces. It can therefore be modelled through an established contact model describing stick–slip behaviour by merely setting the appropriate value for the friction coefficient depending on the contact mechanism (Eq. (10)). Note that this approach ignores tangential lubrication forces between particle pairs that do not explicitly collide, i.e. which remain separated by more than the minimum approach distance $h^{\min}$. Tangential lubrication forces are relatively weak at such distances, justifying this neglect. The value of the lubricated friction coefficient μ_{lub} is not explicitly known. Attempts of Joseph and Hunt [19] to predict the effective coefficient of friction have shown the importance of the local pressure and temperature in the fluid film during the collision. To avoid the need for such elaborate models, the lubricated friction coefficient can be experimentally determined, or estimated. Typically, it can be set one order of magnitude smaller than the dry friction coefficient [19]. In this work, we employed the values reported by Yang and Hunt [16].

$$\mu_f = \begin{cases} \mu_f^{\text{dry}} & \text{if} & h_\sigma^{\min} \ge h_\varepsilon^{\min} \\ \mu_f^{\text{lub}} & \text{if} & h_\sigma^{\min} < h_\varepsilon^{\min} \end{cases} \tag{10}$$

3. Performance

For validation, a binary collision model was implemented in MATLAB, which is available at [25]. The equations of motion were integrated using a velocity Verlet scheme, with a time step equal to 2% of the Hertzian contact time. Collisions corresponding to the work of Yang and Hunt [16] were simulated, and compared with the experimental results. Table 1 lists the used material properties [16]; Fig. 1c defines the geometry of the collisions.

Fig. 2 shows the gap height h during collisions of Delrin spheres at various Stokes numbers. For sufficiently low St, there is no rebound and the particles come to a complete halt at a finite gap height. Beyond a critical St_c, rebound can be seen to increase with increasing St. In their experiments of a moving and a stationary sphere, Yang and Hunt [16] reported noticeable movement of the target when $h = 0.8R^*$.

Table 1
Material properties used for validation [16].

	Steel I	Steel II	Glass	Delrin	
d_p	12.7	12.7	12.7	12.7	mm
ρ_p	7780	7780	2540	1400	kg/m³
Y	190	190	60	2.8	GPa
ν	0.27	0.27	0.23	0.35	–
e_{dry}	0.97	0.97	0.97	0.97	–
σ	24	272	134	796	nm
μ_{dry}	0.11	0.11	0.40	0.20	–
μ_{lub}	0.02	0.02	0.10	0.10	–
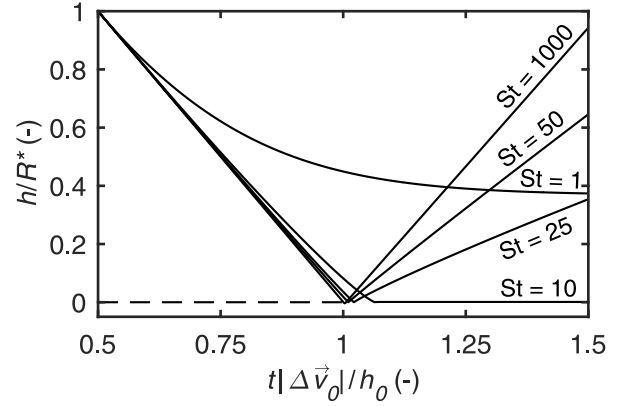
Fig. 2. Evolution of gap height h during collisions of Delrin spheres, at various Stokes numbers.
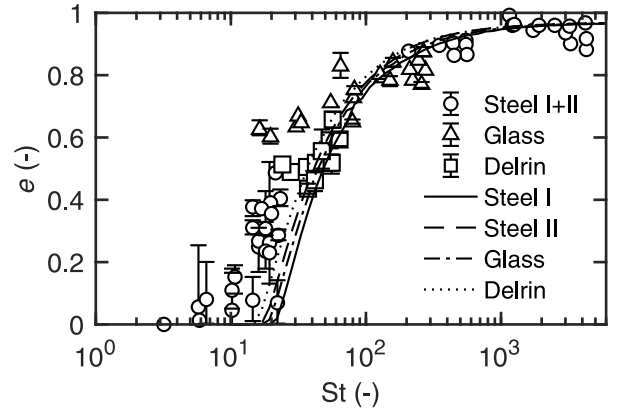
Fig. 3. Coefficient of restitution of head-on collisions for various materials, as a function of the Stokes number. Symbols indicate experimental data by Yang and Hunt [16], with error bars indicating data scatter. Lines indicate results from the current model.

Similar behaviour is observed in the numerical results. At St = 1 the spheres never touch, but interact purely hydrodynamically. This is a good indication that the lubrication force increases the range at which particles influence each other, beyond their physical size.

Fig. 3 shows the coefficient of restitution e during head-on collisions, comparing the current model with the findings of Yang and Hunt [16]. Very similar results were obtained by other groups (e.g. [26, 27]). Clearly, the proposed method captures the trends of the experimental data well. Larger deviations are observed at lower Stokers numbers (St < 20), where Yang and Hunt [16] reported strong experimental scatter due to disturbances in the ambient fluid. Above St = 20, the relative error quickly drops to lower values, below 20%. Similar deviations were found for previous models (e.g. [18]), while these models often rely on fitted, estimated or difficultly measured parameters. The current method thus provides satisfactory accuracy, without the need for such precarious values.
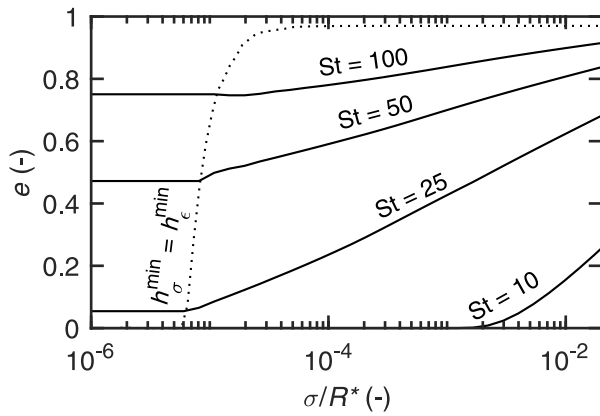
Fig. 4. Influence of surface roughness on the restitution coefficient for head-on collisions of Delrin spheres. Dotted line indicates the condition $h_\sigma^{min} = h_\epsilon^{min}$ for increasing Stokes number.
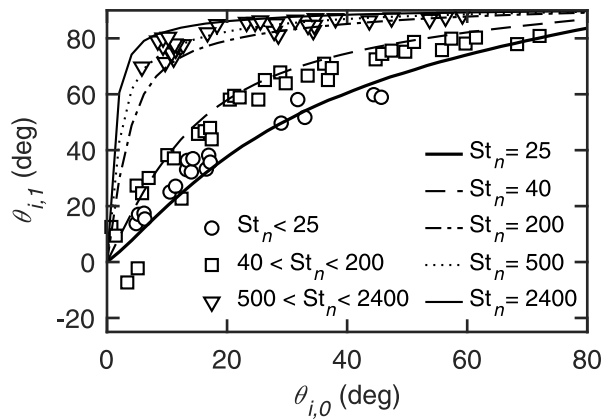

Fig. 5. Angle of rebound $\theta_{i,1}$ of oblique collisions for low ($St_n < 25$, Steel I), intermediate ($40 < St_n < 200$, Delrin) and high ($500 < St_n < 2400$, Steel I) normal Stokes numbers, as a function of the impact angle $\theta_{i,0}$. Symbols indicate experimental data by Yang and Hunt [16], lines indicate results from the current model.

As expected, smoother materials exhibit a higher critical Stokes number, stemming from their smaller minimum approach distance. The importance of the minimum approach distance is further demonstrated by Fig. 4, which shows the restitution coefficient of Delrin spheres as a function of the surface roughness. The influence of surface roughness is strongest in the transitional regime $20 < St < 1000$, where the collision of smoother materials is dampened further. A plateau is reached when $h_\sigma^{min} = h_\epsilon^{min}$ (indicated by the dotted line), when the surfaces deform and the minimum approach distance does not decrease any further. Accounting for this effect greatly improves accuracy, especially for simulation of soft particles and intermediate Stokes numbers.

The model performance during oblique collisions is demonstrated by Fig. 5, which shows impact and rebound angles in three different ranges of the normal Stokes number $St_n = St \cdot \cos(\theta_{i,0})$. The lowest St_n range (conducted in an 80w% glycerol solution) corresponds to elastohydrodynamic collisions, while the two higher ranges (conducted in water) correspond to asperity contact. Dampening of the collisions leads to decreased rebound angles at lower Stokes numbers. Fig. 5 shows good correspondence between numerical and experimental results, especially for the lowest and highest St_n range. Direct comparison for the middle range is precarious, as this range is fairly wide and located around the major transition between viscous and inertial collisions. Considering this, we can only conclude that the current model captures the oblique collisions well.

4. Closing remarks

In this short communication, we have proposed a lubrication force model for future work on unresolved liquid–solid simulations. We have indicated the importance of the interaction distance and surface deformation for accurate representation of immersed collisions. A comparison with experimental results has shown that the current method captures the physics of these collisions very well, while ensuring numerical stability. Therefore, the proposed method is expected to improve accuracy of existing unresolved fluid–solid models. We encourage the scientific community to review the working example of our model published at [25], and assess its applicability for future work.

CRediT authorship contribution statement

Tim M.J. Nijssen: Conceptualization, Methodology, Software, Validation, Formal analysis, Investigation, Data curation, Writing – original draft, Visualization. **Marcel Ottens:** Conceptualization, Writing – review & editing, Supervision, Project administration, Funding acquisition. **Johan T. Padding:** Conceptualization, Methodology, Writing – review & editing, Supervision.

Declaration of competing interest

The authors declare that they have no known competing financial interests or personal relationships that could have appeared to influence the work reported in this paper.

Data availability

The code associated with this work was published and referenced under the Code availability statement.

Code availability

The source code describing the proposed model is openly available at 4TU. ResearchData, published under MIT license [25].

Appendix A. Supplementary data

Supplementary material related to this article can be found online at https://doi.org/10.1016/j.powtec.2022.118017.

References

[1] Z.Y. Zhou, S.B. Kuang, K.W. Chu, A.B. Yu, Discrete particle simulation of particle–fluid flow: model formulations and their applicability, J. Fluid Mech. 661 (2010) 482–510, http://dx.doi.org/10.1017/S002211201000306X.

[2] T. Kempe, J. Fröhlich, Collision modelling for the interface-resolved simulation of spherical particles in viscous fluids, J. Fluid Mech. 709 (2012) 445–489, http://dx.doi.org/10.1017/jfm.2012.343.

[3] J.C. Brändle de Motta, W.P. Breugem, B. Gazanion, J.L. Estivalezes, S. Vincent, E. Climent, Numerical modelling of finite-size particle collisions in a viscous fluid, Phys. Fluids 25 (8) (2013) 083302, http://dx.doi.org/10.1063/1.4817382.

[4] P. Costa, B.J. Boersma, J. Westerweel, W.P. Breugem, Collision model for fully resolved simulations of flows laden with finite-size particles, Phys. Rev. E 92 (5) (2015) 1–14, http://dx.doi.org/10.1103/PhysRevE.92.053012, arXiv:1506.01880.

[5] Y. Xia, H. Xiong, Z. Yu, C. Zhu, Effects of the collision model in interface-resolved simulations of particle-laden turbulent channel flows, Phys. Fluids 32 (10) (2020) 103303, http://dx.doi.org/10.1063/5.0020995.

[6] T.M.J. Nijssen, J.A.M. Kuipers, J. van der Stel, A.T. Adema, K.A. Buist, Complete liquid-solid momentum coupling for unresolved CFD-DEM simulations, Int. J. Multiph. Flow 132 (2020) 103425, http://dx.doi.org/10.1016/j.ijmultiphaseflow. 2020.103425.

[7] G.C. Lopes, X. Bi, N. Epstein, S.A. Baldwin, J.R. Grace, Hydrodynamic characteristics of particles with different roughness and deformability in a liquid fluidized bed, Chem. Eng. Sci. 185 (2018) 50–63, http://dx.doi.org/10.1016/j.ces.2018.03. 058.

[8] G. Liu, F. Yu, S. Wang, P. Liao, W. Zhang, B. Han, H. Lu, Investigation of interstitial fluid effect on the hydrodynamics of granular in liquid-solid fluidized beds with CFD-DEM, Powder Technol. 322 (2017) 353–368, http://dx.doi.org/ 10.1016/j.powtec.2017.08.048.

[9] W. Zhang, R. Noda, M. Horio, Evaluation of lubrication force on colliding particles for DEM simulation of fluidized beds, Powder Technol. 158 (1–3) (2005) 92–101, http://dx.doi.org/10.1016/j.powtec.2005.04.021.

[10] T. Kaluderović Radoičić, M. Duriš, R. Garić-Grulović, Z. Arsenijević, Ž. Grbavčić, Solid circulation rate and particle collisions in quasi two-dimensional water fluidized beds of spherical particles, Powder Technol. 253 (2014) 295–303, http://dx.doi.org/10.1016/j.powtec.2013.11.038.

[11] J.P.F. Campos, K.R.B. Melo, G.C. Lopes, Implementation, validation and application of a lubrication force model in CFD-DEM simulations, Braz. J. Chem. Eng. (2021) 1–12, http://dx.doi.org/10.1007/s43153-021-00134-1.

[12] S. Wang, S. Guo, J. Gao, X. Lan, Q. Dong, X. Li, Simulation of flow behavior of liquid and particles in a liquid-solid fluidized bed, Powder Technol. 224 (2012) 365–373, http://dx.doi.org/10.1016/j.powtec.2012.03.022.

[13] H. Brenner, The slow motion of a sphere through a viscous fluid towards a plane surface, Chem. Eng. Sci. 16 (3–4) (1961) 242–251, http://dx.doi.org/10.1016/ 0009-2509(61)80035-3.

[14] R.G. Cox, H. Brenner, The slow motion of a sphere through a viscous fluid towards a plane surface-II small gap widths, including inertial effects, Chem. Eng. Sci. 22 (12) (1967) 1753–1777, http://dx.doi.org/10.1016/0009-2509(67) 80208-2.

[15] G.G. Joseph, R. Zenit, M.L. Hunt, A.M. Rosenwinkel, Particle–wall collisions in a viscous fluid, J. Fluid Mech. 433 (2001) 329–346, http://dx.doi.org/10.1017/ S0022112001003470.

[16] F.L. Yang, M.L. Hunt, Dynamics of particle-particle collisions in a viscous liquid, Phys. Fluids 18 (12) (2006) 121506, http://dx.doi.org/10.1063/1.2396925.

[17] D. Legendre, R. Zenit, C. Daniel, P. Guiraud, A note on the modelling of the bouncing of spherical drops or solid spheres on a wall in viscous fluid, Chem. Eng. Sci. 61 (11) (2006) 3543–3549, http://dx.doi.org/10.1016/j.ces.2005.12. 028.

[18] F.L. Yang, M.L. Hunt, A mixed contact model for an immersed collision between two solid surfaces, Philos. Trans. R. Soc. Lond. Ser. A Math. Phys. Eng. Sci. 366 (1873) (2008) 2205–2218, http://dx.doi.org/10.1098/rsta.2008.0014.

[19] G.G. Joseph, M.L. Hunt, Oblique particle-wall collisions in a liquid, J. Fluid Mech. 510 (510) (2004) 71–93, http://dx.doi.org/10.1017/S002211200400919X.

[20] R.H. Davis, J.-M. Serayssol, E.J. Hinch, The elastohydrodynamic collision of two spheres, J. Fluid Mech. 163 (1986) 479–497, http://dx.doi.org/10.1017/ S0022112086002392.

[21] C.M. Donahue, C.M. Hrenya, R.H. Davis, Stokes's cradle: Newton's cradle with liquid coating, Phys. Rev. Lett. 105 (3) (2010) 1–2, http://dx.doi.org/10.1103/ PhysRevLett.105.034501.

[22] A. Di Renzo, F.P. Di Maio, Comparison of contact-force models for the simulation of collisions in DEM-based granular flow codes, Chem. Eng. Sci. 59 (3) (2004) 525–541, http://dx.doi.org/10.1016/j.ces.2003.09.037.

[23] M.E. O'Neill, R. Majumdar, Asymmetrical slow viscous fluid motions caused by the translation or rotation of two spheres. Part I: The determination of exact solutions for any values of the ratio of radii and separation parameters, Z. Angew. Math. Phys. ZAMP 21 (2) (1970) 164–179, http://dx.doi.org/10.1007/ BF01590641.

[24] M.E. O'Neill, S.R. Majumdar, Asymmetrical slow viscous fluid motions caused by the translation or rotation of two spheres. Part II: Asymptotic forms of the solutions when the minimum clearance between the spheres approaches zero, Z. Angew. Math. Phys. ZAMP 21 (2) (1970) 180–187, http://dx.doi.org/10.1007/ BF01590642.

[25] T.M.J. Nijssen, M. Ottens, J.T. Padding, Script companion to: A note on the modelling of lubrication forces in unresolved simulations, 2022, http://dx.doi. org/10.4121/19329365.

[26] H.C. Hsu, H. Capart, Enhanced upswing in immersed collisions of tethered spheres, Phys. Fluids 19 (10) (2007) 101701, http://dx.doi.org/10.1063/1. 2771657.

[27] P. Gondret, M. Lance, L. Petit, Bouncing motion of spherical particles in fluids, Phys. Fluids 14 (2) (2002) 643–652, http://dx.doi.org/10.1063/1.1427920.